The Journal of Microbiology, September 2003, p.239-247 Vol. 41, No. 3

Mutational Analysis of an Essential RNA Stem-loop Structure in a Minimal RNA Substrate Specifically Cleaved by *Leishmania* RNA Virus 1-4 (LRV1-4) Capsid Endoribonuclease

Youngtae Ro[1,*] and Jean L. Patterson[2]

[1]*Department of Biochemistry, College of Medicine, Konkuk University, Chungju, Korea 380-701*
[2]*Department of Virology and Immunology, Southwest Foundation for Biomedical Research, San Antonio, Texas 78245-0549*

(Received May 9, 2003 / Accepted June 16, 2003)

The LRV1-4 capsid protein possesses an endoribonuclease activity that is responsible for the single site-specific cleavage in the 5' untranslated region (UTR) of its own viral RNA genome and the formation of a conserved stem-loop structure (stem-loop IV) in the UTR is essential for the accurate RNA cleavage by the capsid protein. To delineate the nucleotide sequences, which are essential for the correct formation of the stem-loop structure for the accurate RNA cleavage by the viral capsid protein, a wild-type minimal RNA transcript (RNA 5' 249-342) and several synthetic RNA transcripts encoding point-mutations in the stem-loop region were generated in an *in vitro* transcription system, and used as substrates for the RNA cleavage assay and RNase mapping studies. When the RNA 5' 249-342 transcript was subjected to RNase T1 and A mapping studies, the results showed that the predicted RNA secondary structure in the stem-loop region using FOLD analysis only existed in the presence of Mg^{2+} ions, suggesting that the metal ion stabilizes the stem-loop structure of the substrate RNA in solution. When point-mutated RNA substrates were used in the RNA cleavage assay and RNase T1 mapping study, the specific nucleotide sequences in the stem-loop region were not required for the accurate RNA cleavage by the viral capsid protein, but the formation of a stem-loop like structure in a region (nucleotides from 267 to 287) stabilized by Mg^{2+} ions was critical for the accurate RNA cleavage. The RNase T1 mapping and EMSA studies revealed that the Ca^{2+} and Mn^{2+} ions, among the reagents tested, could change the mobility of the substrate RNA 5' 249-342 on a gel similarly to that of Mg^{2+} ions, but only Ca^{2+} ions identically showed the stabilizing effect of Mg^{2+} ions on the stem-loop structure, suggesting that binding of the metal ions (Mg^{2+} or Ca^{2+}) onto the RNA substrate in solution causes change and stabilization of the RNA stem-loop structure, and only the substrate RNA with a rigid stem-loop structure in the essential region can be accurately cleaved by the LRV1-4 viral capsid protein.

Key words: *Leishmaniavirus,* endoribonuclease, RNA cleavage, RNA stem-loop structure, metal ion

Leishmaniaviruses are members of the family *Totiviridae,* which persistently infect some strains of the protozoan parasite *Leishmania* (Patterson, 1993). Since the first double-stranded RNA (dsRNA) virus was discovered in *Leishmania* species in 1988 (Tarr *et al.*, 1988), similar viruses have been found in at least 13 strains of *Leishmania.* Of these 13 isolates, full-length cDNA clones have been generated for two New World isolates, LRV1-1 and LRV1-4 (Stuart *et al.*, 1992; Scheffter *et al.*, 1994), and one Old World isolate, LRV2-1 (Scheffter *et al.*, 1995).

The *Leishmania* RNA virus 1-4 (LRV1-4) genome is comprised of an approximately 5.3 kbp of dsRNA with two large open reading frames (ORF2 and ORF3) present on the positive sense strand (Scheffter *et al.*, 1994). When the ORF2 was expressed by a recombinant baculovirus in *Spodoptera frugiperda* cells, the 82-kDa proteins self-assembled into virus-like particles of identical morphology to native virions, demonstrating that the ORF2 encodes the major capsid protein (Cadd and Patterson, 1994). The ORF3 possesses motifs characteristic of viral RNA-dependent RNA polymerase (RDRP), suggesting that it presumably encodes the viral RDRP responsible for the LRV genome transcription and replication (Scheffter *et al.*, 1994). In the genome organization of LRV1-1 and LRV1-4 isolates, the nucleotides at their 5' UTR are highly conserved (90% identity), and it is predicted that five stem-loop structures are conserved in those regions, strongly suggesting that the conserved RNA secondary structure serves an essential viral function (Scheffter *et al.*, 1994; MacBeth and Patterson, 1998).

Since the discovery of a short RNA transcript in both an *in vitro* polymerase assay and in a by-product of the nat-

* To whom correspondence should be addressed.
(Tel) 82-43-840-3739; (Fax) 82-43-851-3944
(E-mail) ytaero@kku.ac.kr

Table 1. Oligonucleotide primers used

Names	Sequences[a] (5'→3')
3'M-342	GGAATTCAAGAAACTTGCTTACG
SL4-BV	ACTCGAGACTGCCGCGAGCGTAAGGNNNTGTT
SL4-SV	ACTCGAGACTGCCGCGAGCGTAAGGGAGNNNTTTG
SL4-LV	ACTCGAGACTGCCGCGAGCGTAAGGGAGTGTTTNNNNAGAC

[a]Viral sequences are underlined and N means a random nucleotide insertion (A, G, C, or T)

ural virus infection in *Leishmania* spp. (Chung *et al.*, 1994), studies have focused on finding the nature of the short transcript and the mapping of the precise cleavage site on the RNA substrate. The cleavage site in the LRV1-4 RNA was previously mapped to the nucleotide 320 of the viral genome, by primer extension analysis to the virus 5' UTR (MacBeth and Patterson, 1995a), and this single-site cleavage responsible for generating the short RNA transcript is mediated by the LRV capsid protein (MacBeth and Patterson, 1995b). Further analysis showed that a stem-loop structure (stem-loop IV) in the viral nucleotide from 249 to 342, stabilized by divalent metal ions, is a minimal essential determinant for accurate RNA cleavage (Ro and Patterson, 2000). Although it is clear that the stem-loop structure is required for an accurate cleavage of the LRV1-4 minimal RNA substrate (Ro and Patterson, 2000), the precise structure determinants within the stem-loop structure and the functional role of divalent metal ions remain to be elucidated.

Here, we examine and delineate the essential nucleotides necessary for the stem-loop structure stabilization and the functional role of the divalent metal ions on the accurate RNA cleavage by LRV1-4 capsid endoribonuclease using point-mutated minimal RNA substrates.

Materials and Methods

Parasite strain and cell culture.

Leishmania guyanensis stock, MHOM/BR/75/M4147 (M-4147), was grown at 23°C in M199 semi-defined medium (Gibco-BRL, USA), supplemented with 5% fresh, filter-sterilized human urine (Armstrong and Patterson, 1994).

Virus purification

The LRV virions were purified as previously described (Chung *et al.*, 1994). Briefly, *Leishmania* promastigotes were harvested at the early stationary phase, washed, and lysed in 1% Triton X-100. The cell lysates were fractionated in a 10 to 40% sucrose gradient, and a fraction containing the most abundant virus particles was selected and used for the *in vitro* RNA cleavage assays.

PCR-directed mutagenesis

The control plasmid used for generating a wild-type minimal RNA substrate, RNA 5'249-342, for the *in vitro* transcription system has been depicted previously (Ro and Patterson, 2000). The parental plasmid, pBSK-Full14, encoding a full-length cDNA copy of the LRV1-4 RNA genome under the control of a T7 transcriptional promoter (Ro *et al.*, 1997), was used as a template for generating a series of point mutants in the stem-loop IV region using PCR-directed random mutagenesis. The pBSK-Full14 was amplified by PCR with *Taq* DNA polymerase (Roche, Germany) and a pair of primers, described in Table 1 and 2, according to the manufacturer's instructions. The PCR products of the expected sizes were captured in the pCRII vector (Invitrogen, USA), and at least ten different colonies having a recombinant plasmid were selected and screened for each mutant group (BV-, SV-, and LV-series mutant group). The plasmids from each clone were purified using a QIAprep spin miniprep kit (Qiagen, USA), and digested with the restriction enzymes, *Xho*I and *Eco*RI (Roche, Germany). The small (approximately 100 bp-sized) *Xho*I/*Eco*RI-digested fragments from each mutant group were gel-purified, combined, and ligated into the large pBSK-Full14 fragment (approximately 7.6 kbp-sized) cut with *Xho*I/*Eco*RI, using T4 DNA ligase (Roche, Germany). The clones with an insert were selected, and the point mutations in the stem-loop region verified by DNA sequencing. The point-mutants used in this study are described and summarized in Table 2.

Synthesis of substrate RNA transcripts

Prior to generating the substrate RNA transcripts for the *in vitro* RNA cleavage assay, the plasmid templates described above were linearized by digestion with *Eco*RI restriction enzyme. The transcription was accomplished in an *in vitro* reaction with T7 RNA polymerase (Promega, USA), according to the manufacturer's protocol. The transcription reaction mixture was incubated at 37°C for 2 h, and the template DNA removed by RQ1 DNase (Promega, USA) with an additional 15 min incubation at 37°C. The transcribed RNAs were then treated with calf intestine phosphatase (NEB, USA) to remove the 5' terminal phosphate.

End-labeling of RNA and purification of labeled RNA

The dephosphorylated RNAs were 5' end-labeled with T4 polynucleotide kinase (NEB, USA) and [γ-^{32}P] ATP (NEN, USA), as previously described (MacBeth *et al.*, 1997). The kinase reaction mixture contained 70 mM

Table 2. Relationship of the predicted stemloop IV structure of mutant RNAs and RNA cleavage

Primers used	Sequences[a] wild	mutated	Names	Predicted secondary structure[b]	RNA cleavage
5'M-249/3'M-342	267GAGUGUUUUGGC278		5'249-342	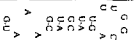	Yes
	^{267}GAG^{269}	^{267}UAG^{269}	BV1	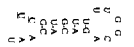	Yes
SL4-BV/3'M-342	^{267}GAG^{269}	^{267}UAG^{269}	BV1	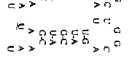	Yes
	^{267}GAG^{269}	^{267}UUU^{269}	BV1	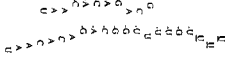	No
	^{270}UGU^{272}	^{270}GGG^{272}	SV6	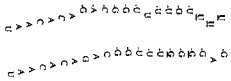	No
	^{270}UGU^{272}	^{270}AGU^{272}	SV7	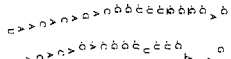	No
SL4-SV/3'M-342	^{270}UGU^{272}	^{270}AGA^{272}	SV10	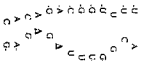	Yes
	^{270}UGU^{272}	^{270}UUG^{272}	SV12	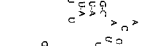	Yes
	^{275}UGGC^{278}	^{275}UUUC^{278}	LV1	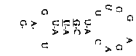	Yes
SL4-LV/3'M-342	^{275}UGGC^{278}	^{275}UUAA^{278}	LV4	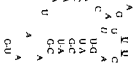	Yes
	^{275}UGGC^{278}	^{275}UAUA^{278}	LV7	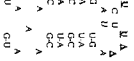	Yes

[a]Mutated nucleotides are highlighted with underline.
[b]Secondary structures of mutant RNAs are predicted by FOLD analysis and nucleotides from 267 to 287 are only shown here.

Tris-HCl (pH 7.6), 10 mM $MgCl_2$, 5 mM dithiothreitol (DTT), 0.6 μM [γ-^{32}P] ATP (6,000 Ci/nmol) and 1 to 15 μM RNA. The mixtures were incubated at 37°C for 2 h, and the phenol/chloroform-extracted RNA fractionated on a 0.4 mm thick 5% polyacrylamide-8.3 M urea gel (National Diagnostic, USA). The RNA was located by UV-shadowing and purified from the gel as previously described (MacBeth *et al.*, 1997).

In vitro RNA cleavage assay

The cleavage assay was performed as previously described (MacBeth and Patterson, 1995a). Briefly, the RNA cleavage activity was assayed in a 20 μl reaction mixture containing the substrate RNA (100,000 cpm), sucrose-purified virus particles and 20 units of the recombinant RNase inhibitor, RNasin (Promega, USA). The mixture was incubated at 37°C for 40 min, and then the reaction was stopped by a phenol/chloroform extraction. A portion of each reaction mixture was mixed with formaldehyde loading dye and heat-denatured at 90°C for 2 min. The reaction products were resolved on a denaturing 6% polyacrylamide-8.3 M urea gel and visualized by autoradiography.

Base-specific RNase mapping analysis

The RNase mapping reactions (10 μl volume), with RNase T1 (Pharmacia, USA) and A (USB, USA), were performed as previously described (Rosenstein and Been, 1991) with minor modifications. Briefly, the reaction mixture contained 200,000 cpm of 5' end-labeled RNA followed by the addition of the diluted RNase (final concentrations are given in the Figure legend). The reaction mixtures with RNase T1 and RNase A contained 40 mM Tris-HCl (pH 8.0), 1 mM EDTA, 0.25 mg/ml yeast tRNA (Sigma, USA) and 0, 2, or 10 mM $MgCl_2$. After incubation for 14 min at 37°C, an equal volume of formamide loading dye was added, and the reactions stored on dry ice until being loaded onto a 10% polyacrylamide-8.3M urea gel. An RNA molecular weight marker was generated by the partial digestion of the 5' end-labeled RNA with RNase T1, according to the manufacturer's protocol. An alkaline hydrolysis ladder was generated by heating the RNA at pH 9.0 for 5 min at 100°C (Donis-Keller *et al.*, 1977).

Electrophoretic mobility shift assay (EMSA)

To check the effect of various reagents on the mobility of the 5' end-labeled RNA, EMSA was performed, as previously described (Bevilacqua and Cech, 1996) with minor modifications. The 5' end-labeled RNA was incubated in binding buffer [25 mM Hepes (pH 7.5), 10 mM NaCl, 5% glycerol, 5 mM DTT, 0.1 mM EDTA and 0.1 mg/ml yeast tRNA] at 37°C, with the various reagents indicated in Fig. 4. After 15 min of incubation, the reaction mixtures were loaded directly onto a 6% (79:1 acrylamide/bis) native gel. The gel and running buffer contained 0.5×TBE [50 mM Tris-base, 41.5 mM boric acid and 1 mM EDTA (final pH 8.3)]. Electrophoresis was performed for 2 h at 20 V/cm at room temperature. The gel was dried, and visualized by autoradiography. For unpaired nucleotide-specific RNase treatments, the RNase A/T1 mixtures were added to the RNA probe reaction mixtures and pre-incubated with 10 mM Mg^{2+} ions for 15 min. After 2 min of incubation at 37°C, the EMSA was performed as described above.

To determine whether the mobility changes caused by

various reagents were due to structural changes of the RNA, RNase T1 digestions were performed by the addition of the enzyme (5×10^{-3} units/μl, final concentration) to a reaction mixture containing 5' end-labeled RNA 5'249-342 and the various reagents (10 mM each, final concentration). The products were analyzed on a 10% polyacrylamide-8.3 M urea gel.

Results

Structural analysis of a minimal RNA substrate, RNA 5'249-342, by RNase mapping

A FOLD analysis (Zuker and Stiegler, 1981) predicted that the RNA 5'249-342 encoding the conserved stem-loop IV (Ro and Patterson, 2000) can form an RNA secondary structure with a 3 nt loop/bulge region (nucleotides from 267 to 269, BV region), followed by a 3 nt base-paired stem region (nucleotides from 270 to 272, SV region) and a 6 nt unpaired hairpin loop (nucleotides from 274 to 279, LV region) (Fig. 1). However, more informative data can be obtained by mapping studies with RNases sensitive to RNA structure in solution (Ehresmann *et al.*, 1987). For examples, RNase T1 cuts after the unpaired guanosine (G) residue (Ehresmann *et al.*, 1987). RNase A cuts after unpaired pyrimidine (C or U) residues, but has a preference for cytidine (C) residues, especially in the sequence context CpA (Knapp, 1989). Also, RNase V1 recognizes portions of the sugar phosphate backbone, which are in a somewhat helical formation (Lowman and Draper, 1986), and can therefore be used to detect either base-paired or stacked residues. The magnesium ion is a required component for many endoribonuclease activities (Deutscher, 1993) including LRV capsid endoribonuclease (MacBeth and Patterson, 1995a). Therefore, it was also of interest to study the effect of divalent metal ions on those aspects of the structure that may be revealed by RNase mapping.

To find the possible secondary structure of RNA 5'249-342 in solution, the 5' end-labeled RNA was individually digested with RNase T1 and A in the presence of increasing Mg^{2+} ion concentrations under native condition. The results showed that in the absence of Mg^{2+} ions, most of the G residues encoded in the RNA 5'249-342 stem-loop region were readily susceptible to cutting by the RNase T1, as shown by comparison with the digestion under denaturing conditions (Fig. 2, lane D and 0), which showed that the proposed secondary structure by a FOLD analysis did not occur in the absence of Mg^{2+} ions. In the presence of Mg^{2+} ions, however, the G280 and G residues in nucleotides from 255 to 271 appeared to be resistant to

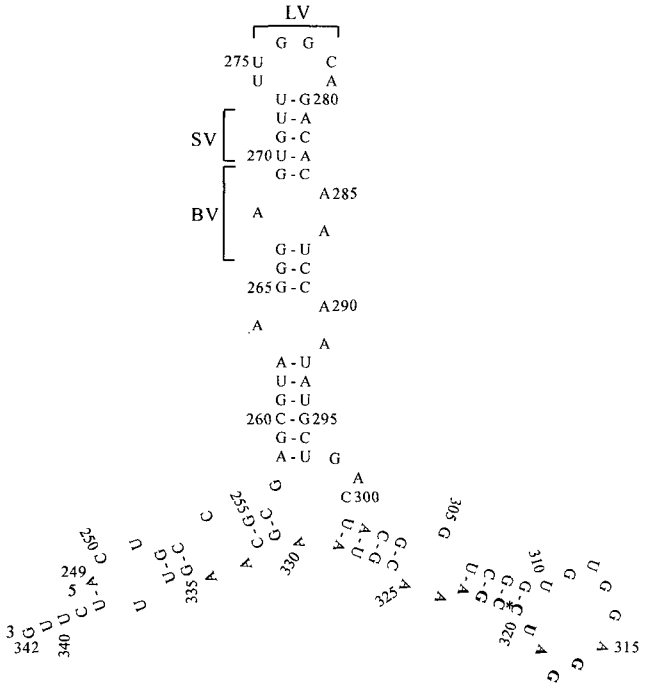

Fig. 1. A predicted secondary structure of RNA 5'249-342. FOLD analysis was used to identify the potential secondary structure encoded in the RNA transcript containing the viral nucleotides from 249 to 342. The regions targeted for mutations are indicated as bulge/loop variables (BV), stem variables (SV) and hairpin loop variables (LV). The number indicates the position of each nucleotide relative to the 5' end of LRV1-4 plus-strand RNA (EMBL/GenBank U01899). A putative consensus RNA cleavage sequence and the cleavage site are shown in boldface and by the asterisk, respectively.

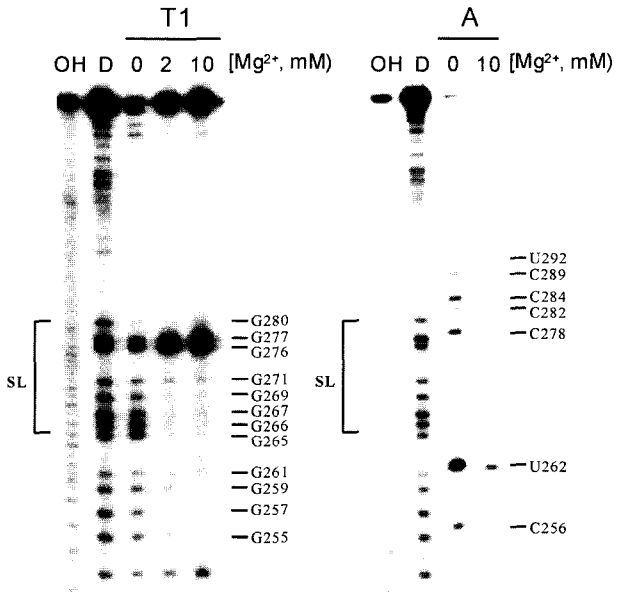

Fig. 2. RNase mapping of RNA 5'249-342. Reaction mixtures, with RNase, contain 0, 2 or 10mM $MgCl_2$, as indicated. The final concentrations of RNase T1 and A used in the reactions were 5×10^{-3} units/μl and 6.4×10^{-5} μg/μl, respectively. The stem-loop region (SL) protected from the single-strand specific RNase, in the presence of Mg^{2+} ions, is shown on the left. A randomly cleaved RNA 5'249-342 ladder was generated by alkaline hydrolysis (OH). The RNA molecular weight marker was generated from the partial digestion of RNA 5'249-342 by RNase T1 (D) under denaturing conditions. The nucleotide positions are indicated on the right.

RNase T1 cutting, and the residues, G276 and G277, appeared to be more susceptible to RNase T1 cutting. The RNase A mapping study also showed similar results to the RNase T1 mapping (Fig. 2), suggesting that a secondary structure predicted by a FOLD analysis matched the RNA secondary structure obtained from the RNase mapping analysis in the presence of Mg^{2+} ions, and that the Mg^{2+} ions stabilized the secondary structure of the stem-loop IV in RNA 5'249-342. The effect of Mg^{2+} ion in the RNase V1 mapping study could not be analyzed, as the RNase V1 requires Mg^{2+} ions for its activity (Lowman and Draper, 1986).

The importance of a stem-loop like structure in RNA 5249-342 for an accurate RNA cleavage.

Using PCR-directed random mutagenesis, ten plasmid

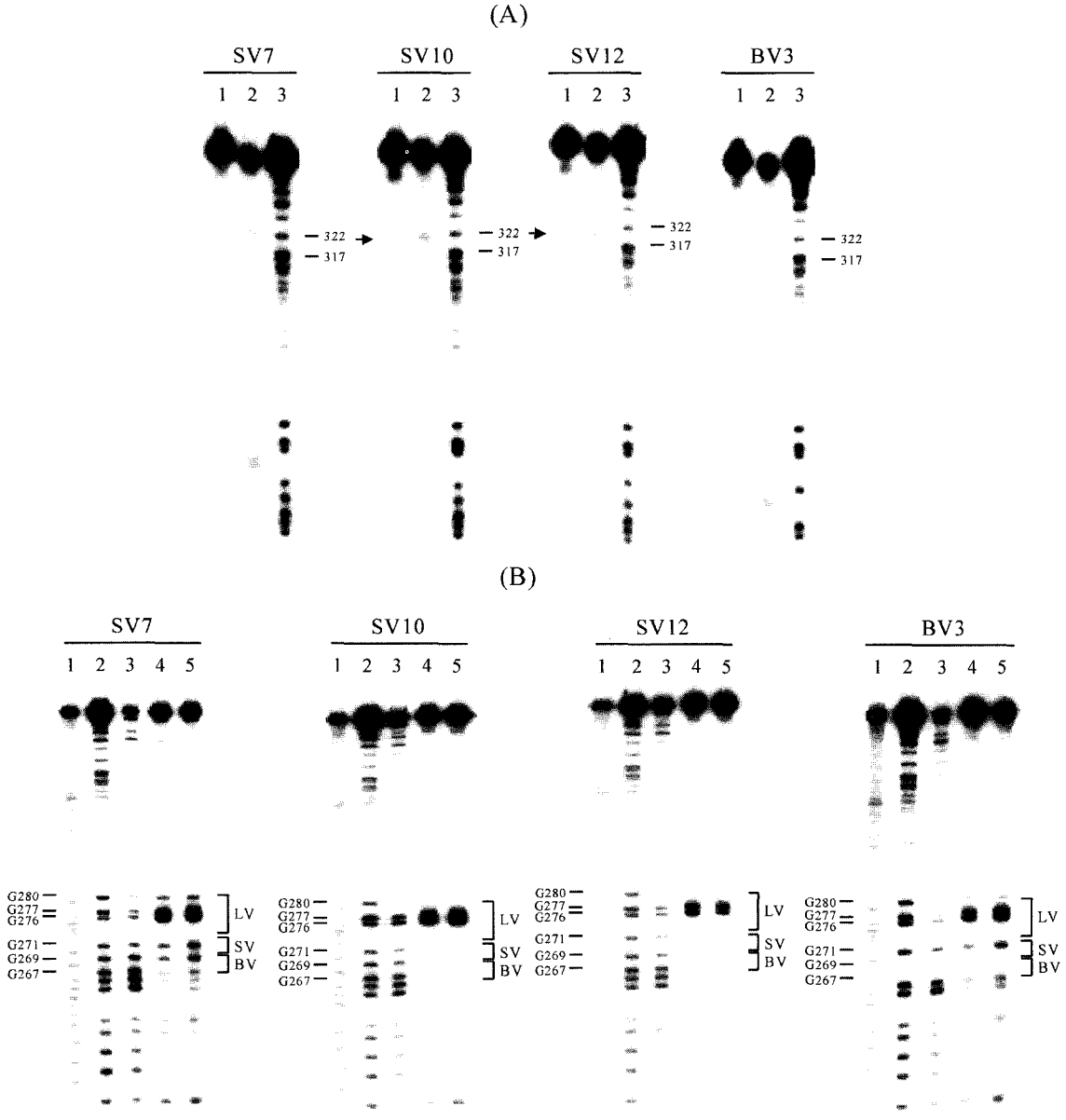

Fig. 3. *In vitro RNA* cleavage assay and RNase T1 mapping of point-mutant RNAs. (A) *In vitro* RNA cleavage assay. The identities of the RNA substrates are indicated above each gel (see Table 2 for detailed description). The indicated 5' end-labeled point mutant RNA transcripts were incubated in the absence (lane 1) or presence (lane 2) of sucrose gradient-purified LRV1-4 viral particles for 40 min. The RNA molecular weight marker was generated from the partial digestion of RNA 5'249-342 by RNase T1 (lane 3). The molecular sizes are indicated as the nucleotide position on the right. An arrow indicates the 320-bp cleavage product. (B) RNase T1 mapping. Reaction mixtures with RNase T1 contain 0 (lane 3), 2 (lane 4), or 10 mM $MgCl_2$ (lane 5). The final concentration of RNase T1 used in the reactions was 5×10^{-3} units/μl. The stem-loop region, proposed in Fig. 1, is shown on the right. A randomly cleaved RNA 5'249-342 ladder was generated by alkaline hydrolysis (lane 1). The RNA molecular weight marker was generated from the partial digestion of RNA 5'249-342 by RNase T1 (lane 2) under denaturing conditions. The nucleotide positions are indicated on the left.

clones, which encoded point mutations in the BV, SV, and LV regions, were isolated (see table 2 for the detailed description). These mutant RNAs were synthesized in an *in vitro* transcription system, and used in the RNA cleavage assay and RNase mapping studies, Two point-mutated RNAs in the BV region, BV1 and BV2, were cleaved by the capsid protein, similarly to the wild-type RNA 5'249-342 (data not shown). The RNase T1 mapping study also revealed that in the presence of Mg^{2+} ions, both the RNAs showed almost identical digestion patterns to those of the RNA 5'249-342 (data not shown), suggesting that their secondary structures, as predicted by FOLD analysis (Table 2), were similar to the wild-type RNA 5'249-342, and that the base changes at the G267 and A268 nucleotides can not disrupt the conserved stem-loop formation and RNA cleavage. However, BV3, another mutant RNA in the BV region, was defective in the accurate RNA cleavage caused by the capsid protein (Fig. 3A). The RNase T1 mapping study of the BV3 RNA interestingly showed that the G280 residue and G residues in the stem-loop region (nucleotides from 267 to 279), which had been resistant to cutting by the RNase T1 in the presence of Mg^{2+} ions, now appeared to be susceptible to RNase T1 cleavage (Fig. 3B), indicating that the stem-loop region was not formed by a single base change from G to U at nucleotide 269. When the SV7 mutant RNA, resistant to cleavage by the capsid protein (Fig. 3A), was subjected to RNase T1 mapping analysis in the presence of Mg^{2+} ions, it showed an almost identical digestion pattern to that in the absence of Mg^{2+} ions (Fig. 3B), indicating that a single base change from U to A at position 270 completely disrupted the stem-loop structure. The SV6 mutant RNA, which encoded the double mutations at nucleotides from 270 and 272, was also resistant to cleavage by the capsid protein, and showed no stem-loop structure in the presence of Mg^{2+} ions similarly to the SV7 mutant RNA analysis (data not shown). A FOLD analysis of two other mutant RNAs in the SV region, SV10 and SV12, predicted that a stem-loop structure can be generated in both RNAs, but the structure was different from that of the original RNA 5'249-342 (Table 2). When both RNAs were subjected to RNA cleavage assay and RNase T1 mapping analysis, the results interestingly showed that both RNAs were susceptible to cleavage by the capsid protein, and that different stem-loop structures were generated in the presence of Mg^{2+} ions (Fig. 3A and B). Three mutant RNAs (LV1, LV4, and LV7) in the LV region were susceptible to cleavage by the capsid protein and RNase T1 mapping study, and also showed that they all had an identical stem-loop structure, which was stabilized by Mg^{2+} ions, to that of the RNA 5'249-342 (data not shown).

Taken together, the RNA cleavage assay and secondary structure analysis from the FOLD analysis and RNase T1 mapping (Table 2) suggest that an accurate RNA cleavage of the substrate RNA 5'249-342 due to the LRV1-4 capsid protein does not require specific nucleotide sequences, but absolutely requires a stem-loop like structure in nucleotides 267 to 287, and that Mg^{2+} ions are essential for stabilizing a stem-loop structure in that region.

Effect of divalent metal ions on the secondary structure of RNA 5'249-342

An EMSA study was performed with RNA 5'249-342 to test whether divalent metal ions can affect the RNA secondary structure changes or RNA folding, as suggested above. The 5' end-labeled RNA probe was incubated with the indicated metal ions and reagents for 15 min at 37°C, and analyzed on a 6% polyacrylamide gel, as described in Materials and Methods. The results indicted that a slow-migrating complex was formed in the reaction mixtures containing divalent metal ions (Mg^{2+}, Ca^{2+}, or Mn^{2+} ions), but not in the mixtures containing ammonium ions or EDTA (Fig. 4A). The slow-migrating complex was not formed when the probe was co-incubated with Mg^{2+} ions and EDTA (data not shown), suggesting that Mg^{2+} ions bind to the probe RNA and change its mobility. To further clarify the nature of the slow-migrating complex, the mobility shift assay mixtures were pre-incubated with or without Mg^{2+} ions for 15 min at 37°C, and then RNase A/T1 mixture was added to the reaction mixtures. After 2 min of incubation at 37°C, the reaction mixtures were directly loaded onto a 6% polyacrylamide gel and analyzed by autoradiography. In the absence of Mg^{2+} ions, the probe was completely degraded in 2 min by a mixture of RNase A/T1 (Fig. 4B). The reason that a little amount of a slow-migrating complex occasionally appeared, even in

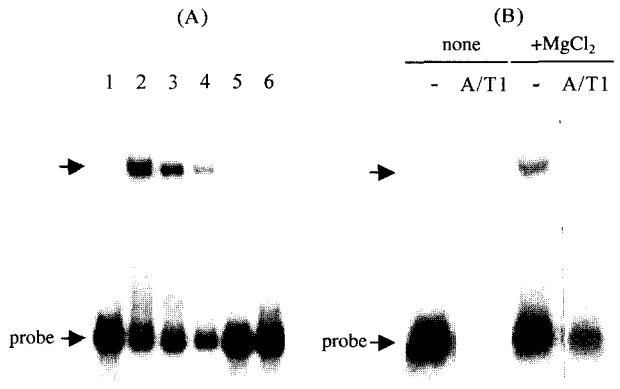

Fig. 4. The effects of the various reagents on the mobility change of RNA 5'249-342. (A) Electrophoretic mobility shift assay (EMSA). Each reagent (10 mM final concentration) was incubated with the 5' end-labeled RNA 5'249-342 probe (100,000 cpm) for 15 min, and the binding mixtures analyzed on a 6% polyacrylamide-8.3 M urea gel. Lanes: no reagent (1), $MgCl_2$ (2), $CaCl_2$ (3), $MnCl_2$ (4), NH_4Cl (5) and EDTA (6). (B) RNase A/T1 cleavage. 5' end-labeled RNA 5'249-342 was pre-incubated with or without 10 mM $MgCl_2$ for 15 min, and then treated with (A/T1) or without (-) RNase A plus T1 mixtures for 2 min. The final concentrations of the RNase A and T1 were 6.4×10^{-5} μg/μl and 5×10^{-3} units/μl, respectively. The products were analyzed as described above. An arrow indicates a slow-migrating complex.

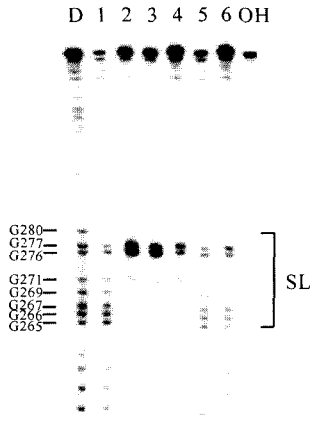

Fig. 5. The effects of the various reagents on the secondary structure of RNA 5'249-342. The RNase T1 digestion under native conditions was performed by the addition of the enzyme (5×10^{-3} units/μl, final concentration) into the reaction mixtures containing the 5' end-labeled RNA 5'249-342 substrate and the various reagents (10 mM final concentration each). The reactions were terminated by the addition of formamide RNA loading dye, and the products analyzed on a 10% polyacrylamide-8.3 M urea gel. Lanes: no reagent (1), $MgCl_2$ (2), $CaCl_2$ (3), $MnCl_2$ (4), NH_4Cl (5) and EDTA (6). A randomly cleaved RNA 5'249-342 ladder was generated by alkaline hydrolysis (OH). The RNA molecular weight marker was generated from the partial digestion of RNA 5'249-342 by RNase T1 (D) under denaturing conditions. The nucleotide positions are indicated on the left and the stem-loop region (SL) on the right.

the absence of Mg^{2+} ions, is unclear (Fig. 4B). Both the RNA probe and the slow-migrating complex formed in the presence of Mg^{2+} ions were also mostly degraded by RNase A/T1 (Fig. 4B), suggesting that the complex contains the unpaired RNA moiety. However, it is noteworthy that they reveal some resistance to RNase A/T1 cutting, demonstrating that Mg^{2+} ions truly affect the structural modification of the RNA 5'249-342.

To further confirm the effects of divalent metal ions on the structural change of the RNA 5'249-342, RNase T1 mapping analysis was performed with the RNA in the presence of the reagents used in the EMSA study (Fig. 5). The reaction mixtures containing divalent metal ions appeared to show the stem-loop region to be resistant to RNase T1 digestion. However, the stem-loop region was susceptible to RNase T1 cutting in reaction mixtures containing ammonium ions or EDTA, suggesting that divalent metal ions are solely required for the stem-loop structure formation. In the presence of divalent metal ions, the digestion patterns of the RNA 5'249-342 caused by the RNase T1 were almost identical. However, it is interesting that the susceptibility to the RNase T1 cutting at nucleotides G276 and G277 in the loop region (LV) was less in the presence of Mn^{2+} ions than those in the presence of Mg^{2+}or Ca^{2+} ions.

Discussion

A finding that the LRV capsid protein acted as an endoribonuclease was quite unprecedented among the known viral capsid proteins, because one of the known major roles of viral capsid proteins is to protect their genomes from nucleases in intracellular and extracellular environments. As the endoribonuclease activity of the capsid protein is conserved in the LRV genus (MacBeth and Paterson, 1995a), it has been suggested that the conserved secondary structure in the 5' UTR of LRV1-1 and LRV1-4 RNA genomes (Scheffter *et al.*, 1994) might provide important viral functions, including RNA cleavage by their own capsid protein. Previously, *in vitro* RNA cleavage assays with the mutant RNA transcripts have revealed the minimal essential sequence for the accurate RNA cleavage resides in the nucleotides from 249 to 342 of the LRV1-4 RNA genome (Ro and Patterson, 2000). Also, RNase mapping studies have shown the conserved stem-loop IV structure definitely exists, and its disruption eliminates the accurate RNA cleavage caused by the viral capsid protein (Ro and Patterson, 2000).

When a possible RNA secondary structure of the minimal RNA transcript, RNA 5'249-342, was predicted by FOLD analysis (Zuker and Stiegler, 1981), the essential stem-loop IV structure retained a stack of two base-paired regions [nucleotides 265-267 and 269-273 (SV)], distorted by an internal adenine (A) loop/bulge region (BV), with a terminal hairpin loop (LV) (Fig. 1). Even though the structure was predicted by a computer program, the presence of the proposed stem-loop structure in solution should be, however, resolved by an RNase mapping study to further delineate the importance of the stem-loop structure on the accurate RNA cleavage caused by the LRV capsid protein. In the absence of Mg^{2+} ion, the stem-loop structure in RNA 5'249-342, obtained by RNase mapping analysis (RNase A, T1, and V1), did not exist as indicated by the FOLD analysis, suggesting that the RNA secondary structure in solution may vary according to the specific experimental conditions. When Mg^{2+} ions were added to the RNA reaction mixture, however, the RNase mapping pattern in the stem-loop region yielded an almost identical structure to that proposed for the stem-loop by the FOLD analysis, indicating that Mg^{2+} ions can enhance and stabilize the formation of the stem-loop structure. Similarly, a potential pseudoknot structure, generated by RNA oligonucleotides *in vitro*, can be transited into two different hairpin structures depending on the experimental conditions, such as the ionic strength, ambient temperatures, metal ions, loop size, or loop sequences (Wyatt *et al.*, 1990).

The effects of divalent metal ions, especially Mg^{2+}, on endoribonucleases and ribozymes could be summarized in their roles in the catalytic activity and/or for stabilizing RNA folding. The highly specific endoribonucleases participating in the RNA processing and turnover require divalent Mg^{2+} ions for their catalysis (Deutscher, 1985). For example, a ribonuclease that specifically degrades

RNA in RNA:DNA hybrid structures require Mg^{2+} ions and the presence of a sulfhydryl reagent, such as DTT, for its maximum activity. The Mg^{2+} ions requirement could only be partially replaced by the Mn^{2+} ions (Berkower *et al.*, 1973). The RNase E processing p5 rRNA in *Escherichia coli* needs Mg^{2+} or Mn^{2+} ions for its activity, but this requirement could not be fulfilled by Ca^{2+} or Zn^{2+} ions (Misra and Apirion, 1978). Another glimpse into the importance of divalent metal ions on the RNA folding are their role(s) in the formation and stabilizing of the three-dimensional structures in many other types of RNA, including tRNA (Bujalowski *et al.*, 1986; Misra and Draper, 2002), *Bacillus subtilis* P RNA (Beebe *et al.*, 1996), the *Tetrahymena* ribozyme RNA (McConnell, *et al*, 1997), and RNA oligomers (Serra *et al.*, 2002).

From the RNase mapping analysis in this study, the Mg^{2+} or Ca^{2+} ions have shown to stabilize the proper folding of a specific region (stem-loop IV) of the RNA 5'249-342. The *in vitro* RNA cleavage studies with mutant RNAs suggest that the proper formation of a stem-loop structure in the nucleotides from 267 to 287 is essential for the accurate RNA cleavage caused by the LRV capsid protein. The structural changes of the stem-loop region in response to point mutations are closely related to loss of the cleavage specificity caused by the capsid protein, suggesting that the stabilized stem-loop structure, driven by divalent metal ions (Mg^{2+} or Ca^{2+} ions), may be essential for the recognition and/or the accurate RNA cleavage by the viral capsid protein. The EMSA study with different chemicals showed that the presence of metal ions (Mg^{2+}, Ca^{2+}, or Mn^{2+} ions) induces a mobility change in the RNA substrate. Mg^{2+} ions also render both the probe RNA and the slow-migrating complex less susceptible to single-strand specific RNase A/T1, suggesting that divalent metal ions bind to the substrate RNA and stabilize the double-stranded RNA structure in the region. However, it remains an open question whether the metal ions are directly involved in the RNA catalysis, as with the other ribozymes.

It is important to note that even though the stem-loop IV region in RNA 5'249-342 is resistant to cleavage by RNase T1 in the presence of Mn^{2+} ions in a similar way to in the presence of Mg^{2+} or Ca^{2+} ions, but the RNase T1 cutting at nucleotides G276 and G277 in the loop region (LV) was less susceptible in the presence of Mn^{2+} ions than in the presence of Mg^{2+} or Ca^{2+} ions. Interestingly, Mn^{2+} ions do not enhance the RNA 5'249-342 cleavage caused by the viral capsid protein (Ro and Patterson, 2000), suggesting that the structural transition of the stem-loop region by Mn^{2+} ions is somewhat different from that by Mg^{2+} or Ca^{2+} ions, and this difference provides no enhancement of the RNA 5'249-342 cleavage caused by the viral capsid endoribonuclease activity. Indeed, the effect of metal ions on the RNA structure may vary depending on the type and concentration of metal ions. For examples, the higher order RNA structure of the self-splicing intron of *Tetrahymena thermophila* produced by Mn^{2+}, Ca^{2+}, or Sr^{2+} ions is similar, but only the Mg^{2+}-stabilized RNA is catalytically active (Celander and Cech, 1991). Also, Mn^{2+} ions at a concentration of 0.1 mM stimulate ribonuclease Q activity, but become inhibitory at higher concentrations (Shimura *et al.*, 1978).

The infection of *Leishmania* cells by LRV is believed to be persistent, as no extracellular particles have ever been observed, and the isolated virions cannot stably infect virus-free *Leishmania* (Armstrong *et al.*, 1993; Patterson, 1993). Even though the exact functional role in the LRV life cycle for the capsid endoribonuclease activity remains to be determined, it was proposed that RNA cleavage is likely to affect the turnover rate of the viral RNA (MacBeth and Patterson, 1998). Recently, it was found that only the fully-assembled LRV1-4 virus particles possess the endoribonuclease activity (unpublished observation), suggesting that the endoribonuclease activity may control the viral copy number in host *Leishmania* cells after viral assembly. Therefore, taken together with the results shown in this work, the LRV capsid endoribonuclease could be suggested to contribute to the control of the viral copy number in host *Leishmania* cells via the metal ion mediated-specific transition of viral RNA genome secondary structure.

Acknowledgement

This work was supported by a research grant for YTR from Konkuk University in 2000.

References

Armstrong, T.C. and J.L. Patterson. 1994. Cultivation of *Leishmania braziliensis* in an economical serum-free medium containing human urine. *J. Parasitol.* 80, 1030-1032.

Armstrong, T.C., M.C. Keenan, G. Widmer, and J.L. Patterson. 1993. Successful transient introduction of *Leishmania* RNA virus into a virally infected and an uninfected strain of *Leishmania*. *Proc. Natl. Acad. Sci. USA* 90, 1736-1740.

Beebe, J.A., J.C. Kurz, and C.A. Fierke. 1996. Magnesium ions are required by *Bacillus subtilis* ribonuclease P RNA for both binding and cleaving precursor $tRNA^{Asp}$. *Biochemistry* 35, 10493-10505.

Berkower, I., J. Leis, and J. Hurwitz. 1973. Isolation and characterization of an endonuclease from *Escherichia coli* specific for ribonucleic acid in ribonucleic acid-deoxyribonucleic acid hybrid structures. *J. Biol. Chem.* 248, 5914-5921.

Bevilacqua, P.C. and T.R. Cech. 1996. Minor-groove recognition of double-stranded RNA by the double-stranded RNA-binding domain from the RNA-activated protein kinase PKR. *Biochemistry* 35, 9983-9994.

Bujalowski, W., E. Graeser, L.W. McLaughlin, and D. Porschke. 1986. Anticodon loop of $tRNA^{Phe}$: structure, dynamics, and Mg^{2+} binding. *Biochemistry* 25, 6365-6371.

Cadd, T.L. and J.L. Patterson. 1994. Synthesis of viruslike particles by expression of the putative capsid protein of *Leishmania* RNA virus in a recombinant baculovirus expression system. *J. Virol.* 68, 358-365.

Celander, D.W. and T.R. Cech. 1991. Visualizing the higher order folding of a catalytic RNA molecule. *Science* 251, 401-407.

Chung, I.K., T.C. Armstrong, and J.L. Patterson. 1994. Identification of a short viral transcript in *Leishmania* RNA virus-infected cells. *Virology* 198, 552-556.

Deutscher, M.P. 1985. *E. coli* RNases: making sense of alphabet soup. *Cell* 40, 731-732.

Deutscher, M.P. 1993. Ribonuclease multiplicity, diversity, and complexity. *J. Biol. Chem.* 268, 13011-13014.

Donis-Keller, H., A.M. Maxam, and W. Gilbert. 1977. Mapping adenines, guanines, and pyrimidines in RNA. *Nucleic Acids Res.* 4, 2527-2538.

Ehresmann C., F. Baudin, M. Mougel, P. Romby, J.P. Ebel, and B. Ehresmann. 1987. Probing the structure of RNAs in solution. *Nucleic Acids Res.* 15, 9109-9128.

Knapp, G. 1989. Enzymatic approaches to probing of RNA secondary and tertiary structure. *Methods Enzymol.* 180, 192-212.

Lowman, H.B. and D.E. Draper. 1986. On the recognition of helical RNA by cobra venom V1 nuclease. *J. Biol. Chem.* 261, 5396-5403.

MacBeth, K.J. and J.L. Patterson. 1995a. The short transcript of *Leishmania* RNA virus is generated by RNA cleavage. *J. Virol.* 69, 3458-3464.

MacBeth, K.J. and J.L. Patterson. 1995b. Single-site cleavage in the 5-untranslated region of *Leishmaniavirus* RNA is mediated by the viral capsid protein. *Proc. Natl. Acad. Sci. USA* 92, 8994-8998.

MacBeth, K.J. and J.L. Patterson. 1998. Overview of the *Leishmaniavirus* endoribonuclease and functions of other endoribonucleases affecting viral gene expression. *J. Exp. Zool.* 282, 254-260.

MacBeth, K.J., Y.T. Ro, L. Gehrke, and J.L. Patterson. 1997. Cleavage site mapping and substrate-specificity of *Leishmaniavirus* 2-1 capsid endoribonuclease activity. *J. Biochem.* 122, 193-200.

McConnell, T.S., D. Herschlag, and T.R. Cech. 1997. Effects of divalent metal ions on individual steps of the *Tetrahymena* ribozyme reaction. *Biochemistry* 36, 8293-8303.

Misra, T.K. and D. Apirion. 1978. Characterization of an endoribonuclease, RNase N, from *Escherichia coli*. *J. Biol. Chem.* 253, 5594-5599.

Misra, V.K. and D.E. Draper. 2002. The linkage between magnesium binding and RNA folding. *J. Mol. Biol.* 317, 507-521.

Patterson, J.L. 1993. The current status of *Leishmania* virus 1. *Parasitol. Today* 9, 135-136.

Ro, Y.T. and J.L. Patterson. 2000. Identification of the minimal essential RNA sequences responsible for site-specific targeting of the *Leishmania* RNA virus 1-4 capsid endoribonuclease. *J. Virol.* 74, 130-138.

Ro, Y.T., S.M. Scheffter, and J.L. Patterson. 1997. Specific in vitro cleavage of a *Leishmania* virus capsid-RNA-dependent RNA polymerase polyprotein by a host cysteine-like protease. *J. Virol.* 71, 8983-8990.

Rosenstein, S.P. and M.D. Been. 1991. Evidence that genomic and antigenomic RNA self-cleaving elements from hepatitis delta virus have similar secondary structures. *Nucleic Acids Res.* 19, 5409-5416.

Scheffter, S., G. Widmer, and J.L. Patterson. 1994. Complete sequence of *Leishmania* RNA virus 1-4 and identification of conserved sequences. *Virology* 199, 479-483.

Scheffter, S.M., Y.T. Ro, I.K. Chung, and J.L. Patterson. 1995. The complete sequence of *Leishmania* RNA virus 2-1, a virus of an Old World parasite strain. *Virology* 212, 84-90.

Serra, M.J., J.D. Baird, T. Dale, B.L. Fey, K. Retatagos, and E. Westhof. 2002. Effects of magnesium ions on the stabilization of RNA oligomers of defined structures. *RNA* 8, 307-323.

Shimura, Y., H. Sakano, and F. Nagawa. 1978. Specific ribonucleases involved in processing of tRNA precursors of *Escherichia coli*. Partial purification and some properties. *Eur. J. Biochem.* 86, 267-281.

Stuart, K.D., R. Weeks, L. Guilbride, and P.J. Myler. 1992. Molecular organization of *Leishmania* RNA virus 1. *Proc. Natl. Acad. Sci. USA* 89, 8596-8600.

Tarr, P.I., R.F. Aline, B.L. Smiley, J. Keithly, and K. Stuart. 1988. LR1: a candidate RNA virus of *Leishmania*. *Proc. Natl. Acad. Sci. USA* 85, 9572-9575.

Wyatt, J.R., J.D. Puglisi, and I. Tinoco Jr. 1990. RNA pseudoknots. Stability and loop size requirements. *J. Mol. Biol.* 214, 455-470.

Zuker, M. and P. Stiegler. 1981. Optimal computer folding of large RNA sequences using thermodynamics and auxiliary information. *Nucleic Acids Res.* 9, 133-148.